Endothelial and Cardiomyocyte PI3Kβ Divergently Regulate Cardiac Remodeling in Response to Ischemic Injury

Xueyi Chen[1,3], Pavel Zhabyeyev[1,3], Abul K. Azad[1], Wang Wang[2,3], Rachel A. Minerath[4], Jessica DesAulniers[1,3], Chad E. Grueter[4], Allan G. Murray[1], Zamaneh Kassiri[2,3], Bart Vanhaesebroeck[5], and Gavin Y. Oudit[1,3,*]

[1]Department of Medicine, [2]Department of Physiology, [3]Mazankowski Alberta Heart Institute, University of Alberta, Edmonton, Canada; [4]Division of Cardiovascular Medicine, Department of Internal Medicine, Francois M. Abboud Cardiovascular Research Center, Fraternal Order of Eagles Diabetes Research Center, University of Iowa, Iowa City, Iowa, USA; [5]University College London Cancer Institute, University College London, London, UK.

Running title: Endothelial and cardiomyocyte PI3Kβ in ischemic hearts

***Corresponding Author:** Gavin Y. Oudit, MD, PhD, FRCP(C), Division of Cardiology, Department of Medicine, Mazankowski Alberta Heart Institute, University of Alberta, Edmonton, Alberta, T6G 2S2, Canada; Phone: (780)-407-8569, Fax: (780)-492-9753. Email: gavin.oudit@ualberta.ca.

Category: Original Article

Word Count: 6889; 7 Figures; 5 Supplementary Tables and Figures.

Abstract

Aims: Cardiac remodeling in the ischemic heart determines prognosis in patients with ischemic heart disease (IHD), while enhancement of angiogenesis and cell survival has shown great potential for IHD despite translational challenges. Phosphoinositide 3-kinase (PI3K)/Akt signaling pathway plays a critical role in promoting angiogenesis and cell survival. However, the effect of PI3Kβ in the ischemic heart is poorly understood. This study investigates the role of endothelial and cardiomyocyte PI3Kβ in post-infarct cardiac remodeling.

Methods and Results: PI3Kβ catalytic subunit-p110β level was increased in infarcted murine and human hearts. Using cell type-specific loss-of-function approaches, we reported novel and distinct actions of p110β in endothelial cells versus cardiomyocytes in response to myocardial ischemic injury. Inactivation of endothelial p110β resulted in marked resistance to infarction and adverse cardiac remodeling with decreased mortality, improved systolic function, preserved microvasculature, and enhanced Akt activation. Cultured endothelial cells with p110β knockout or inhibition displayed preferential PI3Kα/Akt/eNOS signaling that consequently promoted protective signaling and angiogenesis. In contrast, mice with cardiomyocyte p110β-deficiency exhibited adverse post-infarct ventricular remodeling with larger infarct size and deteriorated cardiac function, which was due to enhanced susceptibility of cardiomyocytes to ischemia-mediated cell death. Disruption of cardiomyocyte p110β signaling compromised nuclear p110β and phospho-Akt levels leading to perturbed gene expression and elevated pro-cell death protein levels, increasing the susceptibility to cardiomyocyte death. A similar divergent response of PI3Kβ endothelial and cardiomyocyte mutant mice was seen using a model of myocardial ischemia-reperfusion injury.

Conclusions: These data demonstrate novel, differential, and cell-specific functions of PI3Kβ in the ischemic heart. While loss of endothelial PI3Kβ activity produces cardioprotective effects, cardiomyocyte PI3Kβ is protective against myocardial ischemic injury.

Keywords: Myocardial infarction, PI3Kβ, Remodeling, Angiogenesis, Cardiomyocyte death.

Abbreviations and Acronyms

CM	Cardiomyocyte
MI	Myocardial infarction
IR	Ischemia-reperfusion
IHD	Ischemic heart disease
HF	Heart failure
VEGF	Vascular endothelial growth factor
EC	Endothelial cell
PI3K	Phosphoinositide 3-kinase
PIP_3	Phosphatidylinositol-3,4,5-trisphosphate
eNOS	Endothelial nitric oxide synthase
p110β-Tie2	Endothelial cell-specific p110β-inactivated mice
p110β-αMHC	Cardiac myocyte-specific p110β-inactivated mice
p110βFlx	Control littermates with floxed p110β gene
αMHC-Cre	Mice expressed Cre recombinases driven by αMHC promoter
LAD	Left anterior descending artery
TTC	Triphenyl tetrazolium chloride
TUNEL	Terminal deoxynucleotidyl transferase-mediated dUTP nick-end labeling
HUVECs	Human umbilical vein endothelial cells
HCAECs	Human coronary artery endothelial cells
sip110β	Small interfering RNA against human p110β
s-siRNA	Scrambled small interfering RNA
ANP	Atrial natriuretic peptide
BNP	Brain natriuretic peptide
β-MHC	β-myosin heavy chain
LVESV	Left ventricular end-systolic volume
LVEDV	Left ventricular end-diastolic volume
EF	Ejection fraction
WMSI	Wall motion score index

1. Introduction

Ischemic heart disease (IHD) has a high risk of developing heart failure (HF) with a high morbidity and mortality burden worldwide[1]. Given the high metabolic demands of the heart, disruption of coronary blood flow leads to loss of cardiomyocyte (CM) followed by scar formation, both of which are characteristic changes of myocardial infarction (MI) and ischemia-reperfusion (IR) injury[2, 3]. Hence, improving vascular supply by proangiogenic therapy and preventing CM death can protect the ischemic myocardium. During angiogenesis, various angiogenic signals, such as vascular endothelial growth factor (VEGF), activate quiescent endothelial cells (ECs), which proliferate and differentiate to form microvascular sprouts and ultimately neovessels, rescuing peri-infarct CMs and preventing the transition to HF[4]. Meanwhile, necrosis, apoptosis, and autophagy are major contributors to CM death in ischemic hearts, and the extent of CM loss determines infarct size, cardiac function, and patient outcomes[5].

Phosphoinositide 3-kinase (PI3K) signaling pathways are central determinants of cellular response to injury and play a critical role in promoting angiogenesis and cell survival[6]. Members of the class I_A PI3Ks are composed of a p110 catalytic subunit (α, β, and δ) and a regulatory subunit. Activation of insulin- or growth factor-receptor complexes stimulate PI3Ks which promote the production of phosphatidylinositol-3,4,5-trisphosphate (PIP_3) and plasma membrane recruitment of PIP_3-binding proteins, regulating various cellular responses. VEGF and its receptors signal through PI3Kα/Akt/endothelial nitric oxide synthase (eNOS) pathway in ECs, controlling cell survival, migration, vascular permeability, and vessel sprouting[7-9]. In CMs, PI3Kα/Akt signaling regulates ischemia-driven CM apoptosis, hypertrophy, and contractile function[10, 11].

As a member of the class I_A PI3Ks, PI3K p110β isoform is ubiquitously expressed and was originally considered being functionally redundant because p110β functions are similar to other PI3Ks (p110α and p110γ)[12, 13]. In ECs, p110β activity is lower than p110α, and mice harboring inactivated-p110β ECs display normal vasculature, suggesting a dispensable role of p110β during embryonic vascular development[7]. However, the role of p110β in the response to injury has not been examined. Using genetic murine models, we examined the cell-specific function of p110β in ECs versus CMs in response to myocardial ischemic injury. Here we demonstrate that inhibition of endothelial p110β protects the ischemic heart by

promoting the PI3Kα/Akt/eNOS signaling pathway and angiogenesis, while inhibition of p110β activity in CMs exacerbates the adverse cardiac remodeling post-MI by sensitizing CMs to ischemia-triggered cell death.

2. Methods

2.1 Animal Models and Human Explanted Hearts

Mice with p110β-inactivation under the control of Tie2 promoter-driven conditionally-active Cre recombinase (p110β-Tie2) or α-MHC promoter-controlled constitutively-active Cre (p110β-αMHC) were generated as described[13, 14]. Homozygous littermates $p110\beta^{flox/flox}$ (p110βFlx) mice and mice expressing αMHC-driven Cre (αMHC-Cre) were used as control. Tamoxifen (Sigma-Aldrich) was given to 10-week-old p110β-Tie2 and littermate controls to activate Cre in ECs. Cre deletes exons 21 and 22 from *Pik3cb* (gene encoding p110β), producing a truncated p110β which lacks catalytic activity. Animal experiments were conducted in accordance with the Canadian Council for Animal Care guidelines and the Guide for the Care and Use of Laboratory Animals published by the US National Institutes of Health (revised 2011).

Myocardial infarction was achieved by permanent ligation of the proximal left anterior descending artery (LAD). The ligation or sham surgery was performed on 12-week-old male mice by a technician who was blinded to the genotype[15]. Infarct size was visualized using Triphenyl Tetrazolium Chloride (TTC) (Sigma) staining and Masson's trichrome staining. The procedures for IR surgery with 30-minute occlusion protocol were similar to the MI surgery except that a piece of polyethylene tubing was placed on the LAD to minimize vessel damage[16]. The IR protocol was validated by Evans blue perfusion and electrocardiogram (ECG). Mice were sacrificed with intraperitoneal injection with ketamine (100 mg/kg) and xylazine (10 mg/kg) cocktail, and the heart tissue and bone marrow were collected.

Human tissue from non-failing control hearts and failing post-MI hearts were collected from Human Organ Procurement and Exchange program (HOPE) and Human Explanted Heart Program (HELP) respectively, with ethical approval from the Mazankowski Alberta Heart Institute and the Institutional Ethics Committee[15]. Informed and signed consents were obtained from all participants; and our study conformed to the principles outlined in the Declaration of Helsinki.

2.2 Echocardiography

Noninvasive transthoracic echocardiography was performed on mice anesthetized with 1.5% isoflurane in O_2 using Vevo 3100 (Visualsonics). Conventional measurements and speckle-tracking strain analysis was carried out[15, 17]. Global peak systolic strain was calculated as the average of 6 standard anatomical segments.

2.3 Immunofluorescence

Immunofluorescence staining was performed using established protocols[15]. Wheat Germ Agglutinin (WGA, Invitrogen) staining was performed to outline CMs. Fluorescein-conjugated Lectin (Vectorlabs) intravital perfusion was performed to identify the functional vasculature[15]. Fragmented DNA of apoptotic cells was detected using the DeadEnd Fluorometric Terminal Deoxynucleotidyl Transferase-mediated dUTP Nick-End Labeling (TUNEL) System (Promega) according to instructions.

2.4 EC Culture and Bead Angiogenesis Assay

Human umbilical vein ECs (HUVECs) and human coronary artery ECs (HCAECs, ATCC) were used between passage 3 to 7. ECs cultured to 70-80% confluence were transfected with small interfering RNA against human p110β (sip110β) or scrambled small interfering RNA (s-siRNA) for 48 hours to test the effects of genetic ablation of p110β on ECs. Pharmacological inhibition of p110β using the p110β-specific inhibitor TGX-221 (500 nmol/L, Cayman Chemical) was used on ECs for 48 hours. Cells were starved in basal medium for 5 hours prior to stimulation with 50 ng/ml or 100 ng/ml recombinant human $VEGF_{165}$ (PeproTech) for 10 minutes. Where indicated, cells were pre-incubated with the p110α-specific inhibitor BYL-719 (500 nmol/L, Cayman Chemical) or the Akt inhibitor MK-2206 (1 μmol/L, APExBIO) for 1 hour before VEGF stimulation.

In vitro angiogenesis bead assay of HUVECs/HCAECs was performed as described[15]. The number of sprouts was counted using image analysis software (OpenLab), and at least 30 beads per independent experiment were analyzed.

2.5 Adult CM Isolation, Culture, and Stretching

Adult murine left ventricular CMs were isolated from isoflurane (2%)-anesthetized mice; and the isolated CMs were cultured and stretched as described[18]. Plated CMs were cyclically stretched at 1Hz with an elongation of 5% for 3 hours by Flexcell FX-5000 Tension System (Flexcell International Corp) in serum-free culture medium under a 2% CO_2 and 5% O_2 atmosphere.

2.6 Immunoblotting and Nuclear Fractionation

Immunoblotting and nuclear fractionation was performed as previously described[15, 19]. Histone H3 and GAPDH (Cell Signaling) were used as nuclear and cytosolic markers, respectively.

2.7 RNA Sequencing and TaqMan RT-PCR

RNA isolation and RNA sequencing were performed as described[20]. Total RNAs from LVs (3 LVs/group) were extracted. Data were analyzed using WebGestalt, Protein ANalysis THrough Evolutionary Relationships (PANTHER) classification system (Pantherdb.org), and Ingenuity Pathway Analysis. RNA expression levels were examined by TaqMan real-time polymerase chain reaction (RT-PCR) as described[15]. The expression levels of myocardial disease markers, including atrial natriuretic peptide (*Anp*), brain natriuretic peptide (*Bnp*), and β-myosin heavy chain (*β-Mhc*), were examined.

2.8 Statistical Analysis

Statistical analyses were carried out using SPSS Statistics 24 software, and statistical significance was defined as $p<0.05$ (two sided). Continuous data were presented in scatter plots with mean ± SEM. The differences between two groups were evaluated using independent t-test or Mann-Whitney U test after normality examination. One-way ANOVA or Kruskal-Wallis test with pairwise comparisons were used in studies with more than two groups based on the normality of the data. Survival data were presented as the Kaplan-Meier plots and the log-rank test was used to evaluate the statistical significance.

3. Results

3.1 Akt phosphorylation and p110β are elevated in ischemic hearts

Because of the vital role of cardiac Akt in injury repair[21], we examined the protein levels of Akt in post-MI murine heart and found increased Akt phosphorylation, especially at threonine-308, in the infarct and peri-infarct area (Figure 1A). As one of the upstream regulator of Akt activation, the p110β protein level was assessed next to evaluate the effect of MI on p110β. We observed an increase in p110β level in the infarct and peri-infarct area, and to a lesser extent, in the non-infarct area (Figure 1A). Importantly, explanted human hearts showed largely similar trends of phospho-Akt and p110β levels following MI (Figure 1B), suggesting a conserved mechanism of upregulation of p110β following myocardial ischemia. Immunofluorescence analysis showed that in both murine and human hearts, p110β is expressed in both ECs and CMs, and while p110β was constitutively expressed in ECs, it was highly upregulated and localized to the nuclei in CMs (Figure 1C-D). These findings suggest that p110β could have specific and distinct functions in ECs and CMs. Thus, we examined the function of p110β in ECs and CMs separately in response to MI and myocardial IR injury using genetically modified mice.

3.2 Endothelial PI3Kβ inactivation improves cardiac function and remodeling after MI

To gain insight into the role of endothelial p110β in post-MI remodeling, we generated p110β-Tie2 mice in which endothelial p110β was conditionally and partially deleted, producing truncated p110β protein lacking catalytic activity[13]. Successful genetic inactivation of p110β in p110β-Tie2 was confirmed by PCR analysis with truncated p110β gene expression without affecting hematopoietic cells (Supplementary Figure 1A). Both p110β-Tie2 and littermate control (p110βFlx) mice showed similar body weight, heart weight, LV weight, and levels of p110β, p110α, and phospho-Akt in whole-heart protein extracts (Supplementary Figure 1B-C).

p110β-Tie2 and littermate controls were randomly and blindly assigned to sham operation or MI induction (Supplementary Figure 1D). While sham-operated groups had similar cardiac function, post-MI p110β-Tie2 exhibited higher survival rate (92% vs. 74%) by day 7, with improved post-MI cardiac function reflected by maintained left ventricular end-diastolic and end-systolic dimensions, greater ejection fraction and enhanced regional

systolic function (Figure 2A-B and Supplementary Table 1). Consistent with the preservation of post-MI cardiac function, p110β-Tie2 hearts showed lower expression levels of myocardial disease markers with equivalent hypertrophy in both genotypes (Supplementary Figure 1E-F). While initial post-MI infarct size and apoptotic level were comparable between genotypes, p110β-Tie2 showed reduced infarct expansion on day 7 and absence of post-MI pulmonary edema (Supplementary Figure 1G-I and Figure 2C). Moreover, even though sham-operated hearts and the non-infarct area of post-MI hearts displayed similar vascular density between genotypes, p110β-Tie2 showed increased vascular density in the infarct and peri-infarct areas, confirmed by EC marker staining and lectin *in vivo* perfusion for the detection of functional vessels (Figure 2D). Since PI3K/Akt/eNOS and Erk1/2 pathways are critical mediators of cardioprotection[22], we examined the levels of phospho-Akt and phospho-Erk1/2 and found both were increased in post-MI p110β-Tie2 hearts compared to control, while phospho-eNOS was significantly increased in the infarct and remote areas (Figure 2E). Taken together, these findings demonstrate that catalytic inactivation of endothelial p110β resulted in marked cardioprotection following MI associated with preserved vascular density and increased Akt activation in the ischemic area.

3.3 Loss of PI3Kβ activity promotes VEGF-induced PI3Kα/Akt signaling and angiogenic sprouting in ECs

The VEGF/VEGF receptor axis plays a crucial and well-established role in vascular survival and angiogenesis through PI3Kα/Akt signaling[22, 23]. This was also supported by our findings in human umbilical vein ECs (HUVECs) that Akt activation was required for VEGF-induced angiogenic sprouting using Akt inhibitor (MK-2206), VEGF-stimulated Akt activation largely depended on the activity of PI3Kα as the p110α specific inhibitor (BYL-719) completely abolished the effect of VEGF-induced Akt phosphorylation without affecting p110β and p110α protein levels, and VEGF-induced eNOS activation partially relied on Akt activity (Supplementary Figure 2A-C and Figure 3A). Because of the vital role of PI3Kα in VEGF-induced and Akt-mediated angiogenesis, we hypothesized that selective inactivation of p110β in ECs might upregulate PI3K/Akt signaling via the p110α isoform. We first tested the effects of VEGF on HUVECs with p110β-specific siRNA which showed that abrogation of p110β increased Akt and eNOS phosphorylation upon VEGF stimulation which was

completely blocked by BYL-719 (Supplementary Figure 2D-E). These results suggest that the abrogation of p110β leads to an enhanced activation of PI3Kα/Akt signaling. Next, we studied the effect of pharmacological p110β inhibition in ECs on VEGF-induced Akt/eNOS activation as cardioprotective effects were observed in mice with endothelial-p110β inactivation (p110β-Tie2). Consistent with our animal and p110β-deleted EC data, the p110β specific inhibitor (TGX-221) potentiated VEGF-induced Akt activation in HUVECs, which was completely dependent on intact p110α signaling (Figure 3B-C).

To address whether these effects exist in cardiac ECs, human coronary artery ECs (HCAECs) were examined the effect of p110β inhibition on VEGF/PI3K/Akt signaling. Immunofluorescence analysis confirmed the expression of p110β in cardiac ECs (Supplementary Figure 2F). Consistent with our findings in HUVECs, p110β inhibition in HCAECs resulted in a striking increase in Akt and eNOS phosphorylation upon VEGF stimulation without affecting p110α and p110β protein levels, which were suppressed by p110α inhibition (Figure 3D-E). Since the PI3K/Akt pathway is critical in angiogenesis and increased vasculature was detected in ischemic area in post-MI p110β-Tie2 hearts, we performed the angiogenic bead assay to test the effect of p110β inhibition on angiogenic sprouting in HCAECs. Coinciding with increased Akt activation, p110β inhibition potentiated angiogenic sprouting (Figure 3F). Taken together, these data suggest that inhibiting p110β activity enhances VEGF-mediated Akt activation via the p110α isoform resulting in increased angiogenic response in cardiac ECs.

3.4 Inactivation of PI3Kβ in CMs exacerbates cardiac dysfunction following MI

We next evaluated the role of CM-p110β in post-MI remodeling using p110β-αMHC mice which express kinase-dead p110β specifically in CMs (Supplementary Figure 3A). Analysis of truncated p110β gene expression confirmed the success of p110β inactivation in p110β-αMHC hearts, and the adult p110β-αMHC mice were viable and fertile with comparable body weight to littermate controls-p110βFlx (Supplementary Figure 3B-C). The protein level of p110β was reduced in p110β-αMHC hearts without altering whole-heart baseline phospho-Akt levels (Figure 4A). At day 7 post MI, p110β-αMHC mice exhibited a trend of increased mortality compared to controls (62% vs. 76%), with increased left ventricular dimensions, deteriorated systolic function, and worsened regional systolic function (Figure 4B-C and

Supplementary Table 2). Chamber dimensions and cardiac function did not differ between genotypes in sham-operated groups (Figure 4C and Supplementary Table 2). Littermate controls (p110βFlx) exhibited similar cardiac systolic function as αMHC-Cre mice following sham operation and MI (Supplementary Figure 3D), showing that the αMHC transgene expression alone did not affect post-MI remodeling.

Consistent with worsened cardiac function, p110β-αMHC hearts showed larger infarcted area on days 1 and 7 after MI accompanied by pulmonary edema (Figure 4D and Supplementary Figure 3E). This functional and structural deterioration in post-MI p110β-αMHC hearts was accompanied by increased pathological hypertrophy, reduced coronary microvasculature, and strikingly increased MI-related myocardial inflammation (Figure 4E-G). Importantly, analysis of the canonical Akt signaling pathway displayed comparable pAkt-T308 levels, while phosphorylation of Akt at serine-473 was slightly increased in the peri-infarct area of p110β-αMHC hearts (Figure 4H). These results demonstrate that in striking contrast to p110β function in ECs, loss of p110β activity in CMs resulted in increased susceptibility to ischemic injury and adverse post-MI remodeling illustrating a novel cell-dependent role of PI3Kβ signaling.

3.5 CMs with PI3Kβ deficiency are prone to hypoxia-induced cell death: role of PI3Kβ in the regulation of myocardial gene expression

Given the increase in infarct size in p110β-αMHC hearts, we hypothesized that p110β prevents CM cell death. Immunofluorescence and Western blot analysis demonstrated increased apoptosis in post-MI p110β-αMHC hearts, characterized by elevated apoptotic cell number and cleaved caspase 3 protein levels (Figure 5A). Since CMs are not the only cell types to undergo apoptosis under MI, we combined TUNEL and WGA staining to evaluate apoptotic CMs which confirmed an increase in apoptotic CMs in the infarct and peri-infarct area (Figure 5B). To elucidate the molecular mechanisms underlying the increased susceptibility of p110β-αMHC CMs to apoptosis, we analyzed cell death proteins at baseline in left ventricular samples. Pro-apoptotic proteins, including full-length caspase 3, full-length caspase 8, Bax, and Bak, were upregulated in p110β-αMHC; meanwhile RIP3, a critical determinant of necrosis, but not RIP1, was also upregulated (Figure 5C). To determine the effect of the loss of p110β in CMs, we isolated adult CMs and examined the role of p110β in

hypoxia-induced cell death under cyclic mechanical stretch (Figure 5D). Consistent with normal cardiac structure and function in p110β-αMHC mice, p110β-αMHC and control hearts had comparable numbers of viable CMs after isolation (Supplementary Figure 3F). However, cell viability was decreased in p110β-αMHC CMs compared with control CMs in response to 3-hour cyclical stretch under hypoxic condition (5%O_2) (Figure 5E). In line with these data, we observed higher creatine kinase level in the culture media, a marker of CM cell death, and an increase in the number of apoptotic CMs in p110β-αMHC CMs (Figure 5F-G). Thus, CMs with compromised p110β activity develop an intrinsic susceptibility to cell death in response to acute ischemic and hypoxic stress.

Western blot analysis demonstrated that p110β was present in the nuclear fraction of LVs, and immunostaining on isolated adult CMs confirmed the presence of p110β in the nuclei, and both cytosolic and nuclear fractions were decreased in p110β-αMHC hearts (Figure 6A). Surprisingly, in p110β-αMHC hearts, phospho-Akt level was downregulated in the nuclear fraction, but not in the cytosolic fraction, without alteration in the protein levels of FoxO1 and FoxO3a, which are known down-stream effectors of Akt phosphorylation (Figure 6B). Taken together, these findings indicate that deficiency of CM-p110β results in decreased nuclear Akt phosphorylation which might affect nuclear activity independent of FoxO transcription factors, leading to a pro-cell death phenotype in CMs.

To better define the involvement of p110β in transcriptional control, we performed RNA sequencing to clarify the differences in global gene expression profiles in control and p110β-αMHC LVs, which revealed 1057 up-regulated genes and 838 down-regulated genes in p110β-αMHC hearts, affecting the pathways associated with metabolism, cell cycle, and chemokine signaling (Figure 6C-D). Notably, among the affected genes in the p110β-αMHC hearts, genes associated with cell death were prominently upregulated, while genes related to the regulation of metabolic processes were downregulated (Figure 6E). Among the upregulated genes related to biological processes, cellular processes were altered, while protein tyrosine kinases signaling pathway showed minimal changes (Figure 6F). Moreover, apoptosis and inflammatory signaling pathways were dramatically up-regulated in p110β-αMHC (Figure 6G) which is consistent with our observations demonstrating excessive apoptosis and inflammation in the post-MI p110β-αMHC hearts. Ingenuity Pathway Analysis identified activation of *Creb1*, *Smad3*, *Mkl1*, and *Nr3c2* transcription factors; furthermore,

Smad7, *Tfam*, *Ppara*, and *Klf15* transcription factors were inhibited in p110β-αMHC hearts (Figure 6H). Several of these transcriptional regulators are known to be associated with detrimental post-infarct outcomes (*Mkl1, Nr3c2, Smad,* and *Tfam*), as well as with regulation of cardiac metabolism contributing to infarct healing (*Ppara* and *Klf15*)[24-29]. Our data suggest that PI3Kβ signaling in CM is required for protection against ischemic injury and nuclear Akt contributes to this protection.

3.6 PI3Kβ has divergent effects in ECs and CMs facing ischemia-reperfusion (IR) injury

We next examined whether inactivation of p110β in ECs or CMs would affect cardiac performance after IR injury which comprises of ischemic and reperfusion injury and commonly present in MI patients following myocardial reperfusion treatments[30]. IR injury was performed using 30 minutes of LAD occlusion followed by reperfusion in p110β-Tie2, p110β-αMHC, and control mice. *In vivo* Evans Blue perfusion confirmed the occlusion of the LAD as the affected myocardium remained unstained, and successful reperfusion was confirmed when this area was perfused with the dark blue dye stain after the release of LAD obstruction (Figure 7A). Furthermore, bipolar surface electrocardiogram obtained from these mice showed prolonged QRS and elevated ST-segment after 30 min of LAD occlusion compared to baseline electrocardiogram (Figure 7B), indicating the presence of myocardial ischemia. Myocardial strain analysis revealed better longitudinal peak systolic strain in the p110β-Tie2 mice at day 7 post-IR compared to control (Figure 7C). Consistent with improved cardiac function, p110β-Tie2 mice exhibited higher coronary density in the ischemic and peri-ischemic myocardium (Figure 7D). In contrast, at 7-day post-IR, p110β-αMHC mice displayed deteriorated cardiac function with decreased longitudinal peak systolic strain (Figure 7E). In addition, TUNEL staining of 3-hour post-reperfusion hearts revealed increased apoptotic CMs in p110β-αMHC hearts (Figure 7F). These results clearly support the use of myocardial strain analysis to detect changes in cardiac performance and demonstrate that endothelial inactivation of p110β is cardioprotective against IR injury while p110β deficiency in CMs enhances the susceptibility to IR injury.

4. Discussion

Our findings reveal a novel, critical, and cell specific role of p110β in the regulation of endothelial sprouting and CM survival in ischemic hearts. Using EC- and CM-specific p110β-inactivated mice which display comparable cardiac function under physiological conditions, we demonstrate that p110β plays distinct cell-specific roles in the ischemic heart. Specifically, inactivation of endothelial p110β enhances VEGF-stimulated PI3Kα/Akt/eNOS signaling and angiogenesis, reducing myocardial ischemic injury *in vivo*, whereas CM-specific p110β ablation disrupts cellular homeostasis with a pro-cell death profile, sensitizing CMs to cell death following myocardial ischemia (Figure 7G). In the heart, p110β is expressed in ECs and CMs and is upregulated following MI in both murine and human hearts confirming the PI3Kβ signaling pathway is altered in heart disease.

In striking contrast to the dispensable role of endothelial p110β in adult quiescent cardiac vasculature[7], EC-specific p110β inactivation leads to increased Akt phosphorylation, myocardial microvasculature preservation, cardiac function maintenance, and reduced mortality after ischemic injury. Activation of endothelial Akt/eNOS pathway is essential in VEGF-induce postnatal angiogenesis by regulating cell survival, migration, and NO release[8, 31, 32]. Interestingly, despite that endothelial p110α drives the VEGF-induced Akt phosphorylation and following angiogenesis, the reduction or inhibition of p110β in HUVECs enhances VEGF-induced PI3Kα/Akt activation and, to a lesser extent, eNOS activation, improving angiogenic sprouting. The short-term endothelial p110β inhibition has no influence on VEGF-induced Akt activation[7, 33]. However, studies on p110α- or p110β-dependent cancer cells have revealed time-dependent activation of PI3K/Akt signaling in response to dominant-PI3K isoform inhibition by relieving the feedback inhibition of dominant-PI3K isoform on another isoform[34, 35] . Similarly, our results suggest that inhibition of p110β in ECs relieves feedback inhibition of p110β on p110α amplifying VEGF-induced Akt activation and angiogenic sprouting after MI, leading to reduced infarct size, protected cardiac function, and reduced mortality.

Similarly to EC-p110β, CM-p110β is not required for postnatal cardiac development[36]. However, in response to myocardial ischemia, in contrast to the cardioprotective effects of endothelial p110β inactivation, we observe that inactivation of p110β in myocytes sensitizes them to cell death in response to ischemic injury, leading to adverse cardiac remodeling and

deteriorated cardiac function. In line with our observation that considerable nuclear-p110β were present in the CMs, cytosolic p110β/p85β complexes are known to enter the nucleus where they play a role in protecting cells against oxidative stress-induced apoptosis and regulating DNA replication and repair[37-39]. In this framework, inactivation and/or reduction in levels of nuclear p110β should promote oxidative stress-induced apoptosis and hinder DNA repair facilitating cell death increasing size of infarct. In addition, CM-p110β deficiency significantly affects the transcriptional profile of the myocardium characterized by altered the expression of metabolic genes and increased the expression of programmed cell death genes, leading to increase in pro-cell death protein levels, including caspase 3, caspase 8, Bax, Bak, and RIP3, which are associated with adverse outcomes in ischemic hearts by promoting CM death and increasing infarct size[5, 40, 41]. In line with this framework, cardiac overexpression of p110β mediates cardioprotective effects in mice with MI by reducing hypoxia-induced CM apoptosis with increased Akt activation[42]. In this study, we found that overall Akt activation is largely unaffected by p110β deficiency either at quiescent or infarcted state, which is in line with prevailing view that p110β is not required for postnatal cardiac development[36]. However, nuclear Akt activation is diminished in p110β deficient mice, suggesting that nuclear fraction of p110β/Akt contributes to the adverse post-MI outcomes in the model. The cardioprotective function of nuclear p110β may be mediated via Akt, which is known to have multiple roles in the nucleus, such as promoting cell survival and regulating cell cycle[43]. Specifically, in the heart, nuclear accumulation of Akt inhibits CM apoptosis, protecting the heart against IR injury[44].

Overall, our study highlights that p110β is a versatile PI3K isoform in the heart where it has distinct roles in the cardiac endothelium versus cardiomyocytes. Inactivation of p110β in the cardiac endothelium protects the heart from ischemic injury by promoting PI3Kα/Akt signaling and angiogenesis, whereas inactivation of p110β in CMs promotes ischemia-induced cell death by disrupting gene programs and increasing pro-cell death protein levels.

Funding and Acknowledgment

This work was supported by operating grants from the Canadian Institutes of Health Research (CIHR) and Heart and Stroke Foundation to GY Oudit. This study was supported by the American Heart Association (AHA 13SDG14660064, CEG) and NIH (R01 HL125436, CEG). Ms. Xueyi Chen is funded by Li Ka Shing Sino-Canadian Exchange Program.

Conflict of Interest: None declared.

References

1. Roth GA, Nguyen G, Forouzanfar MH, Mokdad AH, Naghavi M, Murray CJ. Estimates of global and regional premature cardiovascular mortality in 2025. *Circulation* 2015;**132**:1270-1282.
2. St John Sutton MG, Sharpe N. Left Ventricular Remodeling After Myocardial Infarction - Pathophysiology and Therapy. *Circulation* 2000;**101**:2981-2988.
3. Yellon DM, Hausenloy DJ. Myocardial reperfusion injury. *The New England journal of medicine* 2007;**357**:1121-1135.
4. Ferrara N, Kerbel RS. Angiogenesis as a therapeutic target. *Nature* 2005;**438**:967-974.
5. Chiong M, Wang ZV, Pedrozo Z, Cao DJ, Troncoso R, Ibacache M, Criollo A, Nemchenko A, Hill JA, Lavandero S. Cardiomyocyte death: mechanisms and translational implications. *Cell death & disease* 2011;**2**:e244.
6. Datta SR, Brunet A, Greenberg ME. Cellular survival: a play in three Akts. *Genes & development* 1999;**13**:2905-2927.
7. Graupera M, Guillermet-Guibert J, Foukas LC, Phng LK, Cain RJ, Salpekar A, Pearce W, Meek S, Millan J, Cutillas PR, Smith AJ, Ridley AJ, Ruhrberg C, Gerhardt H, Vanhaesebroeck B. Angiogenesis selectively requires the p110alpha isoform of PI3K to control endothelial cell migration. *Nature* 2008;**453**:662-666.
8. Ackah E, Yu J, Zoellner S, Iwakiri Y, Skurk C, Shibata R, Ouchi N, Easton RM, Galasso G, Birnbaum MJ, Walsh K, Sessa WC. Akt1/protein kinase Balpha is critical for ischemic and VEGF-mediated angiogenesis. *The Journal of clinical investigation* 2005;**115**:2119-2127.
9. Dimmeler S, Dernbach E, Zeiher AM. Phosphorylation of the endothelial nitric oxide synthase at ser-1177 is required for VEGF-induced endothelial cell migration. *FEBS letters* 2000;**477**:258-262.
10. Matsui T, Tao J, del Monte F, Lee KH, Li L, Picard M, Force TL, Franke TF, Hajjar RJ, Rosenzweig A. Akt activation preserves cardiac function and prevents injury after transient cardiac ischemia in vivo. *Circulation* 2001;**104**:330-335.
11. Crackower MA, Oudit GY, Kozieradzki I, Sarao R, Sun H, Sasaki T, Hirsch E, Suzuki a, Shioi T, Irie-Sasaki J, Sah R, Cheng HM, Rybin VO, Lembo G, Fratta L, Oliveira-dos-Santos AJ, Benovic JL, Kahn CR, Izumo S, Steinberg SF, Wymann MP, Backx PH, Penninger JM. Regulation of Myocardial Contractility and Cell Size by Distinct PI3K-PTEN Signaling Pathways. *Cell* 2002;**110**:737-749.
12. Heller R, Chang Q, Ehrlich G, Hsieh SN, Schoenwaelder SM, Kuhlencordt PJ, Preissner KT, Hirsch E, Wetzker R. Overlapping and distinct roles for PI3Kbeta and gamma isoforms in S1P-induced migration of human and mouse endothelial cells. *Cardiovascular research* 2008;**80**:96-105.
13. Guillermet-Guibert J, Bjorklof K, Salpekar A, Gonella C, Ramadani F, Bilancio A, Meek S, Smith AJ, Okkenhaug K, Vanhaesebroeck B. The p110β isoform of phosphoinositide 3-kinase signals downstream of G protein-coupled receptors and is functionally redundant with p110γ. *Proceedings of the National Academy of Sciences of the United States of America* 2008;**105**:8292-8297.
14. McLean BA, Zhabyeyev P, Patel VB, Basu R, Parajuli N, DesAulniers J, Murray AG, Kassiri Z, Vanhaesebroeck B, Oudit GY. PI3Kalpha is essential for the recovery from Cre/tamoxifen cardiotoxicity and in myocardial insulin signalling but is not required for normal myocardial contractility in the adult heart. *Cardiovascular research* 2015;**105**:292-303.
15. Wang W, McKinnie SM, Patel VB, Haddad G, Wang Z, Zhabyeyev P, Das SK, Basu R, McLean B, Kandalam V, Penninger JM, Kassiri Z, Vederas JC, Murray AG, Oudit GY. Loss of Apelin exacerbates myocardial infarction adverse remodeling and

ischemia-reperfusion injury: therapeutic potential of synthetic Apelin analogues. *Journal of the American Heart Association* 2013;**2**:e000249.
16. Xu Z, Alloush J, Beck E, Weisleder N. A murine model of myocardial ischemia-reperfusion injury through ligation of the left anterior descending artery. *Journal of visualized experiments : JoVE* 2014;**86**:51329.
17. Bauer M, Cheng S, Jain M, Ngoy S, Theodoropoulos C, Trujillo A, Lin F, Liao R. Echocardiographic Speckle-Tracking Based Strain Imaging for Rapid Cardiovascular Phenotyping in Mice. *Circulation research* 2011;**108**:908-916.
18. Li D, Wu J, Bai Y, Zhao X, Liu L. Isolation and culture of adult mouse cardiomyocytes for cell signaling and in vitro cardiac hypertrophy. *Journal of visualized experiments : JoVE* 2014.
19. Dimauro I, Pearson T, Caporossi D, Jackson MJ. A simple protocol for the subcellular fractionation of skeletal muscle cells and tissue. *BMC research notes* 2012;**5**:513.
20. Hall DD, Ponce JM, Chen B, Spitler KM, Alexia A, Oudit GY, Song LS, Grueter CE. Ectopic expression of Cdk8 induces eccentric hypertrophy and heart failure. *JCI insight* 2017;**2**:e92476.
21. Sussman MA, Volkers M, Fischer K, Bailey B, Cottage CT, Din S, Gude N, Avitabile D, Alvarez R, Sundararaman B, Quijada P, Mason M, Konstandin MH, Malhowski A, Cheng Z, Khan M, McGregor M. Myocardial AKT: the omnipresent nexus. *Physiological reviews* 2011;**91**:1023-1070.
22. Simons M, Gordon E, Claesson-Welsh L. Mechanisms and regulation of endothelial VEGF receptor signalling. *Nature reviews Molecular cell biology* 2016;**17**:611-625.
23. Lee S, Chen TT, Barber CL, Jordan MC, Murdock J, Desai S, Ferrara N, Nagy A, Roos KP, Iruela-Arispe ML. Autocrine VEGF signaling is required for vascular homeostasis. *Cell* 2007;**130**:691-703.
24. Small EM, Thatcher JE, Sutherland LB, Kinoshita H, Gerard RD, Richardson JA, Dimaio JM, Sadek H, Kuwahara K, Olson EN. Myocardin-related transcription factor-a controls myofibroblast activation and fibrosis in response to myocardial infarction. *Circulation research* 2010;**107**:294-304.
25. Fraccarollo D, Berger S, Galuppo P, Kneitz S, Hein L, Schutz G, Frantz S, Ertl G, Bauersachs J. Deletion of cardiomyocyte mineralocorticoid receptor ameliorates adverse remodeling after myocardial infarction. *Circulation* 2011;**123**:400-408.
26. Euler-Taimor G, Heger J. The complex pattern of SMAD signaling in the cardiovascular system. *Cardiovascular research* 2006;**69**:15-25.
27. Kunkel GH, Chaturvedi P, Tyagi SC. Mitochondrial pathways to cardiac recovery: TFAM. *Heart failure reviews* 2016;**21**:499-517.
28. Finck BN. The PPAR regulatory system in cardiac physiology and disease. *Cardiovascular research* 2007;**73**:269-277.
29. McConnell BB, Yang VW. Mammalian Kruppel-like factors in health and diseases. *Physiological reviews* 2010;**90**:1337-1381.
30. Hausenloy DJ, Yellon DM. Myocardial ischemia-reperfusion injury: a neglected therapeutic target. *The Journal of clinical investigation* 2013;**123**:92-100.
31. Morello F, Perino A, Hirsch E. Phosphoinositide 3-kinase signalling in the vascular system. *Cardiovascular research* 2009;**82**:261-271.
32. Lee MY, Luciano AK, Ackah E, Rodriguez-Vita J, Bancroft TA, Eichmann A, Simons M, Kyriakides TR, Morales-Ruiz M, Sessa WC. Endothelial Akt1 mediates angiogenesis by phosphorylating multiple angiogenic substrates. *Proceedings of the National Academy of Sciences of the United States of America* 2014;**111**:12865-12870.
33. Haddad G, Zhabyeyev P, Farhan M, Zhu LF, Kassiri Z, Rayner DC, Vanhaesebroeck B, Oudit GY, Murray AG. Phosphoinositide 3-kinase β mediates microvascular endothelial repair of thrombotic microangiopathy. *Blood* 2014;**124**:2142-2149.
34. Costa C, Ebi H, Martini M, Beausoleil SA, Faber AC, Jakubik CT, Huang A, Wang Y, Nishtala M, Hall B, Rikova K, Zhao J, Hirsch E, Benes CH, Engelman JA.

Measurement of PIP3 levels reveals an unexpected role for p110beta in early adaptive responses to p110alpha-specific inhibitors in luminal breast cancer. *Cancer cell* 2015;**27**:97-108.
35. Schwartz S, Wongvipat J, Trigwell CB, Hancox U, Carver BS, Rodrik-Outmezguine V, Will M, Yellen P, de Stanchina E, Baselga J, Scher HI, Barry ST, Sawyers CL, Chandarlapaty S, Rosen N. Feedback suppression of PI3Kalpha signaling in PTEN-mutated tumors is relieved by selective inhibition of PI3Kbeta. *Cancer cell* 2015;**27**:109-122.
36. Lu Z, Jiang YP, Wang W, Xu XH, Mathias RT, Entcheva E, Ballou LM, Cohen IS, Lin RZ. Loss of cardiac phosphoinositide 3-kinase p110 alpha results in contractile dysfunction. *Circulation* 2009;**120**:318-325.
37. Kumar A, Redondo-Munoz J, Perez-Garcia V, Cortes I, Chagoyen M, Carrera AC. Nuclear but not cytosolic phosphoinositide 3-kinase beta has an essential function in cell survival. *Molecular and cellular biology* 2011;**31**:2122-2133.
38. Marques M, Kumar A, Poveda AM, Zuluaga S, Hernandez C, Jackson S, Pasero P, Carrera AC. Specific function of phosphoinositide 3-kinase beta in the control of DNA replication. *Proceedings of the National Academy of Sciences of the United States of America* 2009;**106**:7525-7530.
39. Kumar A, Fernandez-Capetillo O, Carrera AC. Nuclear phosphoinositide 3-kinase beta controls douoble-strand break DNA repair. *PNAS* 2010;**107**:7491-7496.
40. Condorelli G, Roncarati R, Ross J, Jr., Pisani A, Stassi G, Todaro M, Trocha S, Drusco A, Gu Y, Russo MA, Frati G, Jones SP, Lefer DJ, Napoli C, Croce CM. Heart-targeted overexpression of caspase3 in mice increases infarct size and depresses cardiac function. *Proceedings of the National Academy of Sciences of the United States of America* 2001;**98**:9977-9982.
41. Luedde M, Lutz M, Carter N, Sosna J, Jacoby C, Vucur M, Gautheron J, Roderburg C, Borg N, Reisinger F, Hippe HJ, Linkermann A, Wolf MJ, Rose-John S, Lullmann-Rauch R, Adam D, Flogel U, Heikenwalder M, Luedde T, Frey N. RIP3, a kinase promoting necroptotic cell death, mediates adverse remodelling after myocardial infarction. *Cardiovascular research* 2014;**103**:206-216.
42. Lin Z, Zhou P, von Gise A, Gu F, Ma Q, Chen J, Guo H, van Gorp PR, Wang DZ, Pu WT. Pi3kcb links Hippo-YAP and PI3K-AKT signaling pathways to promote cardiomyocyte proliferation and survival. *Circulation research* 2015;**116**:35-45.
43. Martelli AM, Tabellini G, Bressanin D, Ognibene A, Goto K, Cocco L, Evangelisti C. The emerging multiple roles of nuclear Akt. *Biochimica et biophysica acta* 2012;**1823**:2168-2178.
44. Shiraishi I, Melendez J, Ahn Y, Skavdahl M, Murphy E, Welch S, Schaefer E, Walsh K, Rosenzweig A, Torella D, Nurzynska D, Kajstura J, Leri A, Anversa P, Sussman MA. Nuclear targeting of Akt enhances kinase activity and survival of cardiomyocytes. *Circulation research* 2004;**94**:884-891.

Figure Legends

Figure 1. Catalytic isoform of PI3Kβ-p110β is increased in post-MI murine and human hearts and expressed both in ECs and CMs. (A,B) Western blot analysis of Akt and p110β levels on 7-day post-sham/MI mouse hearts and on non-failing control (NFC) and post-MI failing human hearts. *p<0.05 vs. sham/normal hearts, n=3-6 hearts/group (one-way ANOVA). **(C,D)** Immunofluorescence images of p110β (green) in the heart with EC marker-CD31 (red, left panels), WGA outlining CMs (red, right panels), and DAPI marking nuclei (blue) on mouse and human hearts. n=3-4 hearts/group.

Figure 2. Inactivation of endothelial p110β protects the heart against MI by preserving vasculatures and increasing Akt activity in the ischemic areas. (A) Kaplan-Meier survival curve of p110β-Tie2 and p110βFlx mice following MI surgery. *p<0.05, n=36-50 mice/group (log-rank test). **(B)** Echocardiographic images showing ventricular morphology and analysis of left ventricular end-systolic and end-diastolic volume (LVESV and LVEDV), ejection fraction (EF), and wall motion score index (WMSI). *p<0.05 vs. sham, #p<0.05 vs. p110βFlx, n=10 mice/group (one-way ANOVA). **(C)** Infarct size analysis from triphenyl tetrazolium chloride (TTC)-stained sections and representative images of trichrome histological staining of hearts. *p<0.05 vs. p110βFlx, n=5 mice/group (t test). **(D)** Immunofluorescence analysis of EC marker-CD31 (red) and EC marker-lectin (green) via *in vivo* perfusion method on p110β-Tie2 and p110βFlx hearts, with quantification of percentage of fluorescence positive area in different areas. *p<0.05 vs. sham, #p<0.05 vs. p110βFlx, n=3 mice/group (one-way ANOVA). **(E)** Western blot analysis of Akt, Erk1/2, and NOS protein levels in the infarct, peri-infarct, and non-infarct areas from 7-day post-MI hearts. *p<0.05 vs. p110βFlx, n=6-7 mice/group (t test).

Figure 3. Inhibition of p110β in ECs elevates VEGF-stimulated PI3Kα/Akt/eNOS signaling, promoting angiogenesis. (A) Western blot analysis of p110β, p110α, GAPDH, Akt, and eNOS in BYL-719-treated HUVEC lysates. *p<0.05, n=5 independent experiments (one-way ANOVA). **(B)** Western blots demonstrating the effect of VEGF on p110β, p110α, GAPDH, Akt, and eNOS protein levels in TGX-221-treated HUVECs. *p<0.05, n=5

independent experiments (one-way ANOVA). **(C)** Western blot analysis of Akt and eNOS in TGX-221-treated HUVECs with and without BYL-719. *p<0.05, n=5 independent experiments (t test). **(D)** Western blot analysis of p110β, p110α, GAPDH, Akt, and eNOS in HCAECs. *p<0.05, n=5 independent experiments (one-way ANOVA). **(E)** Western blot analysis of Akt and eNOS in TGX-221-treated HCAECs with and without BYL-719. *p<0.05, n=5 independent experiments (t test). **(F)** Representative beads and quantification of sprout number in control and TGX-221-treated HCAECs. *p<0.05, n=5 independent experiments (t test).

Figure 4. CM-specific inactivation of p110β exacerbates cardiac dysfunction after MI, resulting in adverse ventricular remodeling. (A) Western blot analysis of p110β and Akt levels in p110β-αMHC and p110βFlx left ventricular lysates. *p<0.05, n=6-7 mice/group (t test). **(B)** Kaplan-Meier survival analysis in post-MI p110β-αMHC and control mice. n=34-54 mice/group (log-rank test). **(C)** Echocardiographic images showing left ventricular morphology and functional analysis of left ventricular end-systolic and end-diastolic volume (LVESV and LVEDV), ejection fraction (EF), and wall motion score index (WMSI). *p<0.05 vs. sham, #p<0.05 vs. p110βFlx, n=9-10 mice/group (one-way ANOVA). **(D)** Trichrome histological-stained images and triphenyl tetrazolium chloride (TTC)-stained images and infarct size quantification on post-MI hearts. *p<0.05, n=4-7 mice/group (t test). **(E)** Wheat Germ Agglutinin (WGA, green) immunofluorescence staining outlining CM size. *p<0.05 vs. sham, #p<0.05 vs. p110βFlx, n=3 mice/group (one-way ANOVA). **(F)** Vascular density and capillary-to-CM ratio testing by CD31 (red) and WGA (green) immunofluorescence staining on post-surgery hearts. *p<0.05 vs. sham/indicated group, #p<0.05 vs. p110βFlx, n=3 mice/group (one-way ANOVA or t test). **(G)** Neutrophils identified by Ly6B (red, left panels) and macrophages marked by CD68 (red, right panels) immunofluorescence staining on post-MI hearts. *p<0.05, n=3 mice/group (t test). **(H)** Western blot analysis of Akt protein level in 7-day post-MI hearts. *p<0.05 vs. p110βFlx, n=5-7 mice/group (t test).

Figure 5. Inactivation of CM-p110β sensitizes CMs to cell death by increasing pro-cell death proteins expression, leading to increased post-MI cell death. (A) Terminal deoxynucleotidyl transferase-mediated dUTP nick-end labeling (TUNEL, green) and DAPI

(blue) immunofluorescence analysis for apoptotic cells (n=3 mice/group) and western blot analysis for cleaved caspase 3 (n=4 mice/group) on 1-day post-MI hearts. *p<0.05 (t test). **(B)** Combined wheat Germ Agglutinin (WGA, red), TUNEL, and DAPI immunofluorescence staining to highlight apoptotic CMs. *p<0.05, n=3 mice/group (t test). **(C)** Western blot analysis for baseline protein levels of full-length caspase 3, full-length caspase 8, Bax, Bak, RIP1, and RIP3 in left ventricle lysates from p110β-αMHC and control mice. *p<0.05, n=6-7 mice/group (t test). **(D)** Study design for isolated adult CM stretching under hypoxic condition for 3 hours, n=3-4 experiments/group (2 hearts/experiment). **(E)** Representative right field images and cell viability evaluation after stretching. *p<0.05 (t test). **(F)** Evaluation of creatine kinase level in media from cultured CMs. *p<0.05 (t test). **(G)** TUNEL staining from apoptotic CMs (green) with F-actin (red) staining. *p<0.05 (t test).

Figure 6. p110β is expressed in CM nuclei and CM-p110β inactivation alters gene expression in the heart. (A) Nuclear fractionation analysis for p110β, GAPDH and Histone H3 in p110β-αMHC and p110βFlx left ventricular lysates and immunofluorescence images of p110β (green) and sarcomeric α actin (red) on isolated murine CMs. *p<0.05, n=6 mice/group (t test). **(B)** Fractionation analysis for Akt, FoxO1, and FoxO3a in p110β-αMHC and p110βFlx left ventricular lysates. *p<0.05, n=6 mice/group (t test). **(C)** Scatterplot of significantly differentially-expressed genes after RNA-seq analysis on p110β-αMHC and p110βFlx left ventricles. n=3 mice/group. **(D)** KEGG pathway enrichment analysis of RNA-seq results for significantly altered genes. **(E)** WebGestalt enrichment analysis for disrupted pathways on significantly upregulated and downregulated genes in biological processes. **(F)** Panther GO analysis showing subcategories of differential gene expression in biological processes. **(G)** Significantly altered signaling pathways identified by Panther signal transduction pathways analysis. **(H)** Potentially altered upstream transcription factors identified by Ingenuity Pathway Analysis.

Figure 7. Divergent role of p110β in ECs and CMs in response to myocardial IR injury. (A) Sequential images of IR surgery with Evans Blue perfusion showing the blue dye rushes into the infarcted area after the release of occlusion. **(B)** Representative electrocardiogram (ECG) of mice with IR surgery. **(C)** Echocardiographic longitudinal strain analysis on 7-day

post-IR p110β-Tie2 and control mice with representative longitudinal strain curve images. *p<0.05, n=5-6 mice/group (t test). **(D)** Vascular density evaluated by staining EC marker-CD31 (red) on 7-day post-IR hearts. *p<0.05 vs. p110βFlx, n=3 mice/group (t test). **(E)** Echocardiographic longitudinal strain analysis and representative longitudinal strain curve on 7-day post-IR p110β-αMHC and control hearts. *p<0.05, n=6-7 mice/group (t test). **(F)** Representative immunofluorescence images of terminal deoxynucleotidyl transferase-mediated dUTP nick-end labeling (TUNEL, green) staining with Wheat Germ Agglutinin (WGA, red) showing apoptotic CMs on 3-hour post-IR hearts. *p<0.05, n=3-4 mice/group (t test). **(G)** Schematic diagram depicting the functions of p110β in cardiac ECs and CMs in response to ischemic injury. Disruption of EC-p110β signaling enhances PI3Kα/Akt activation in the ischemic heart, promoting angiogenesis, while nuclear PI3Kβ/Akt in CMs is required to maintain cellular homeostasis to prevent cell death facing ischemic stress.

Figure 1

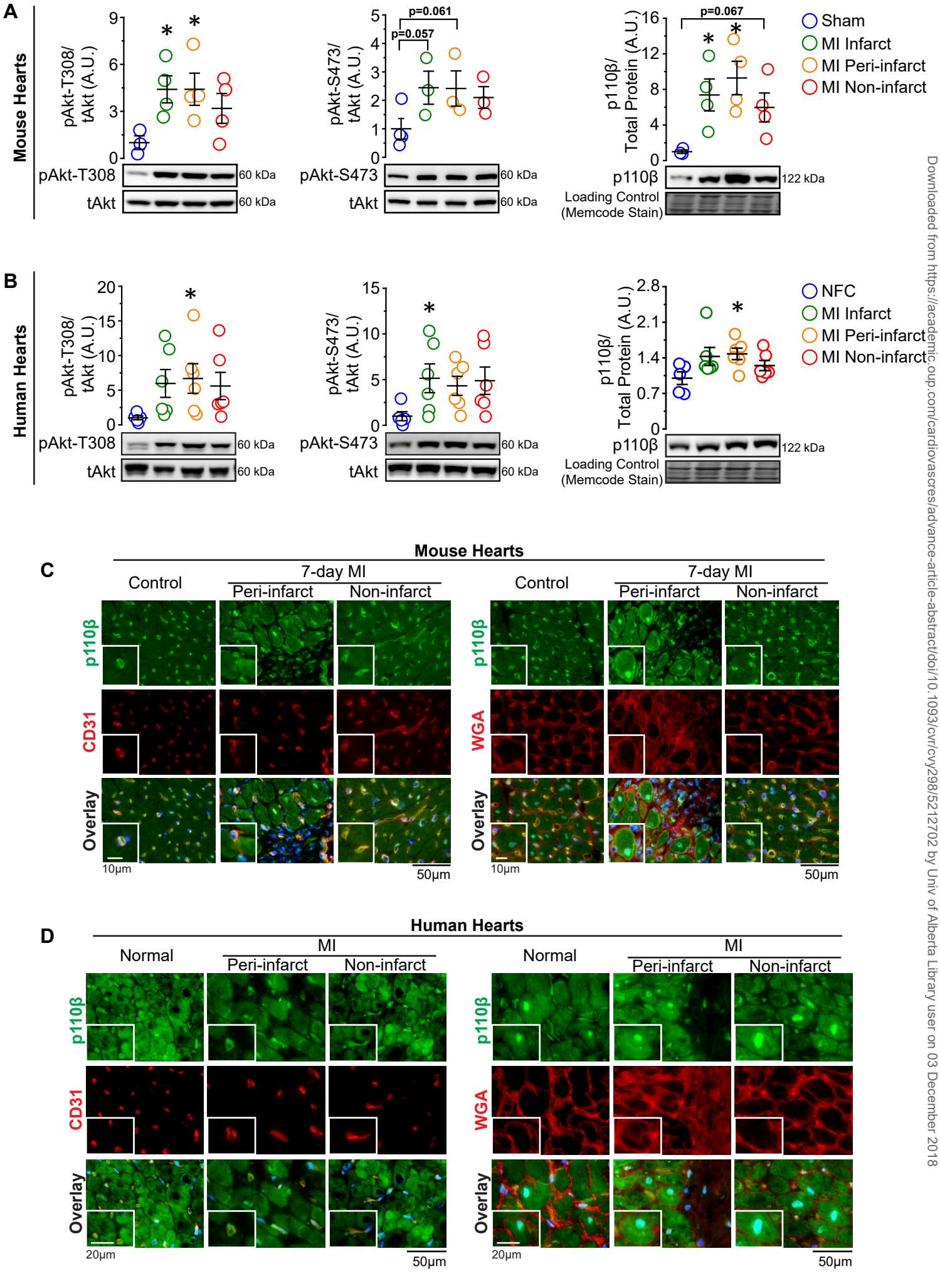

Chen, X. et al. Figure 1

Figure 2

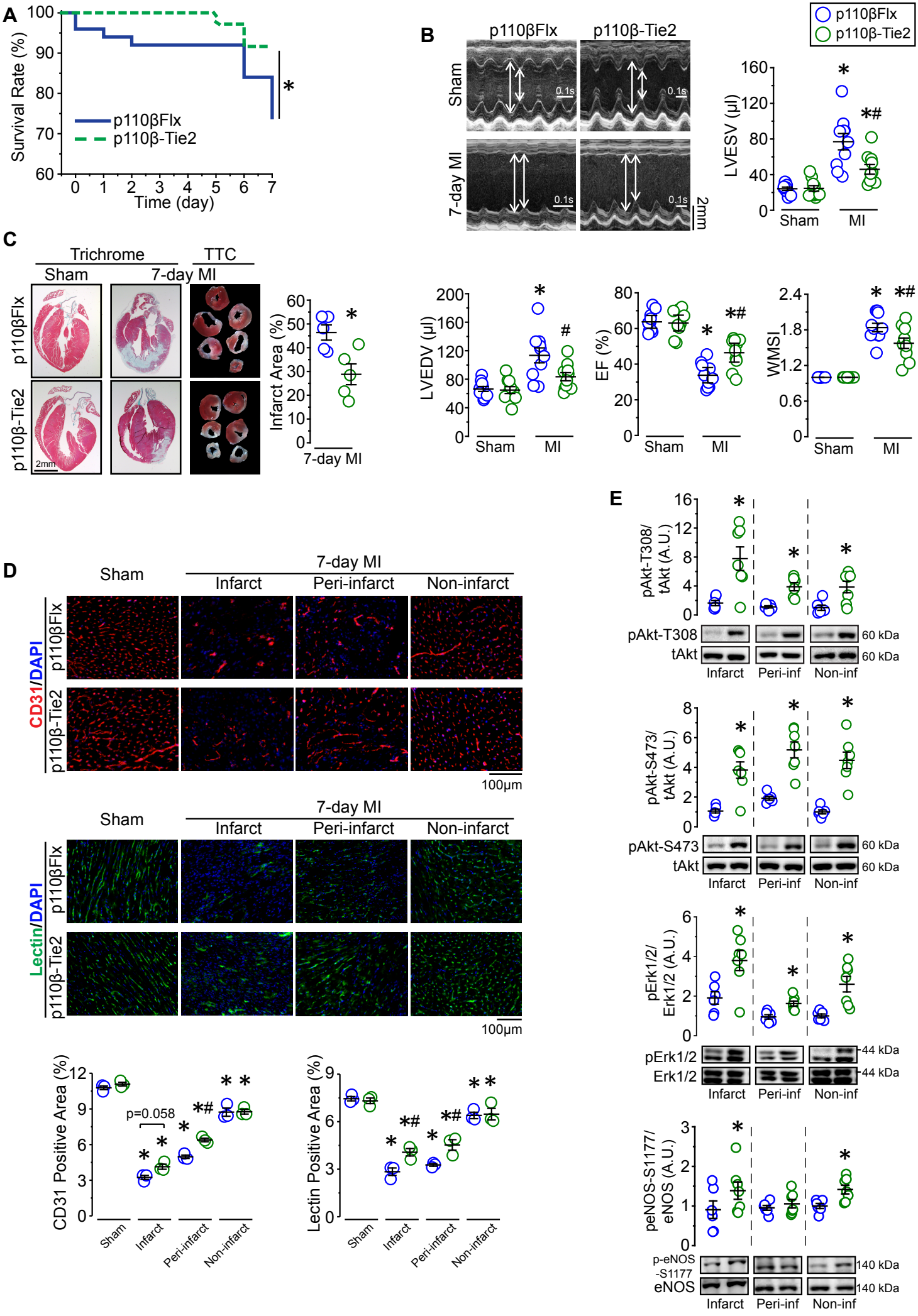

Chen, X. et al. Figure 2

Figure 3

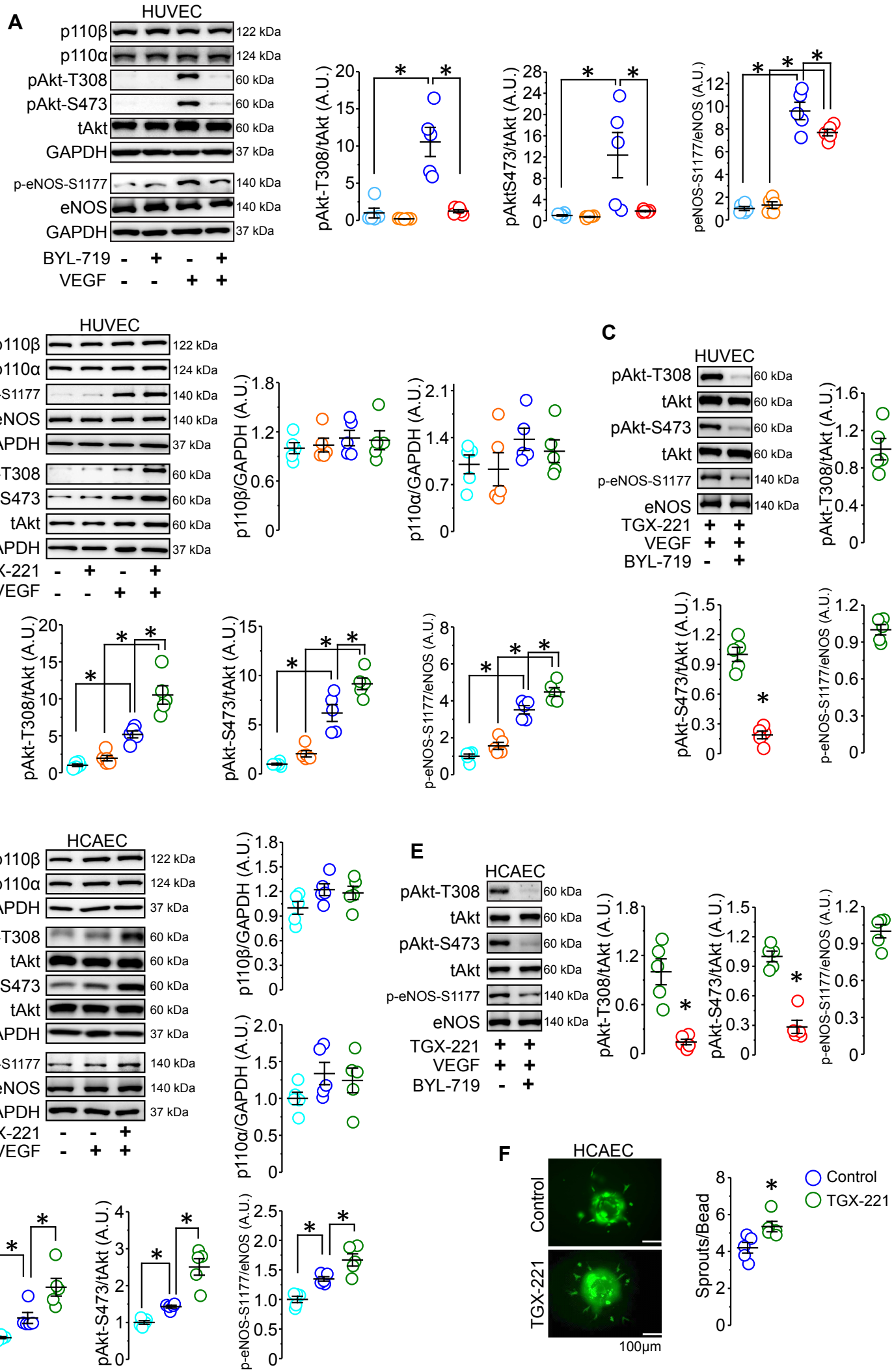

Chen, X. et al. Figure 3

Figure 4

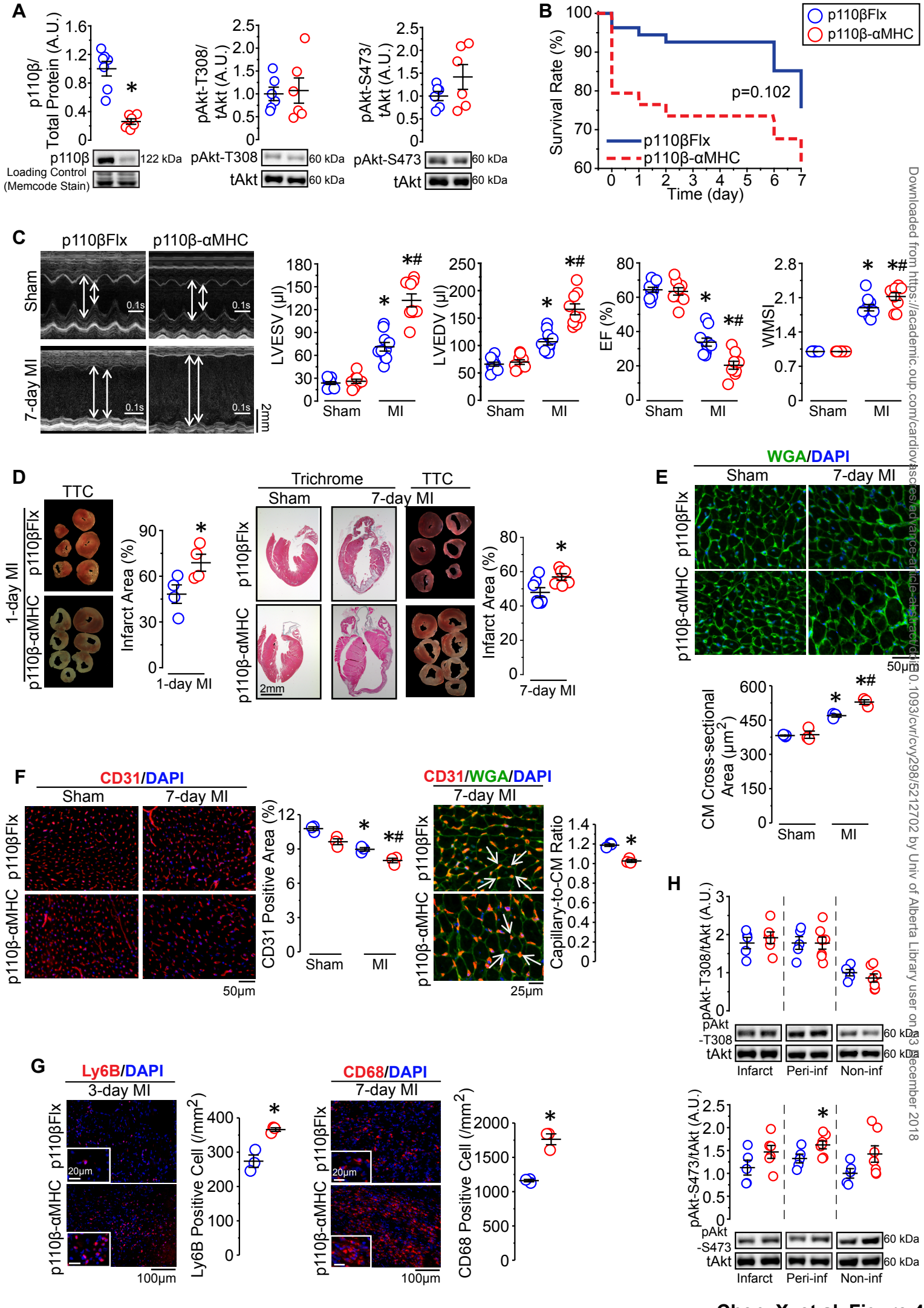

Chen, X. et al. Figure 4

Figure 5

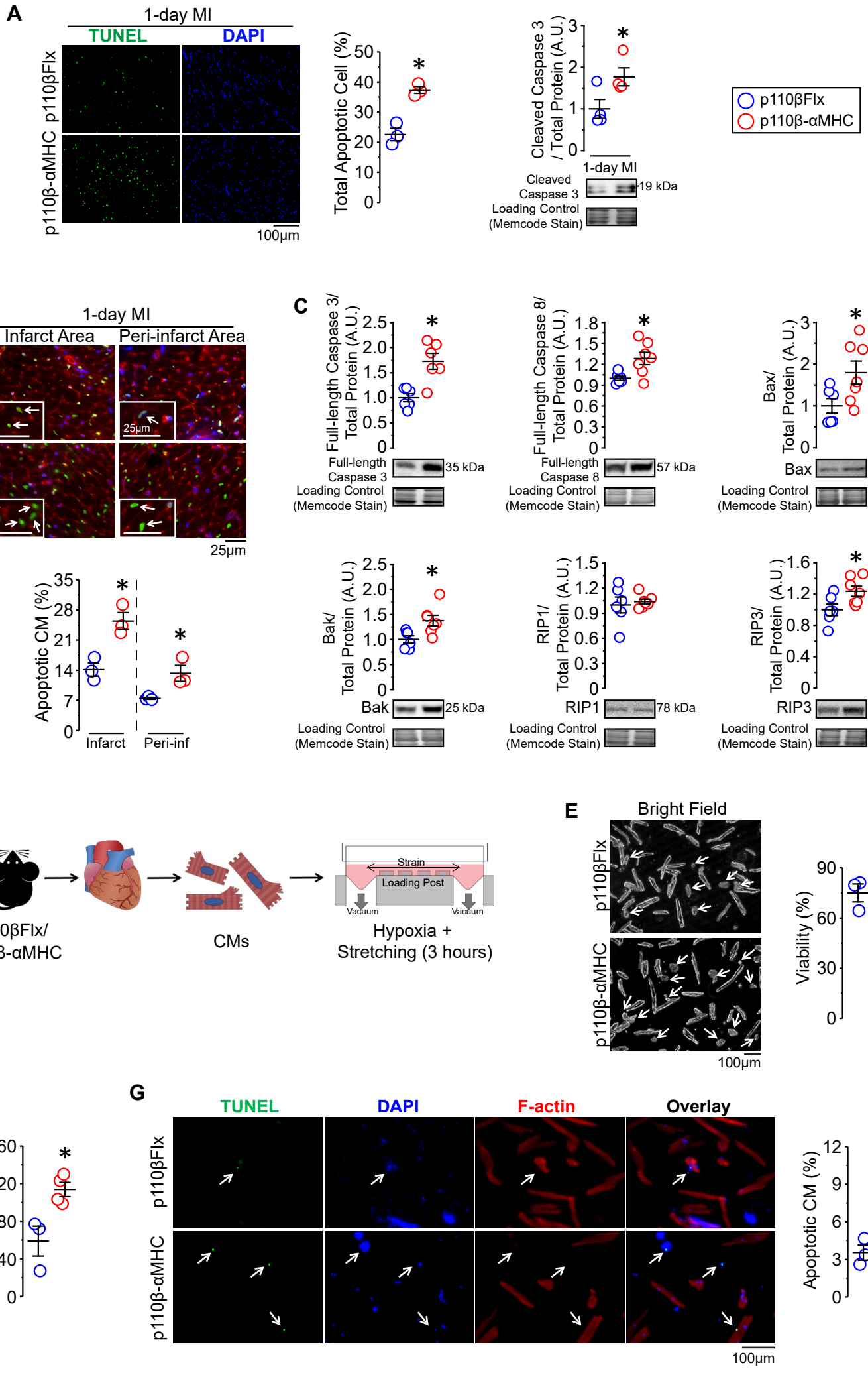

Figure 6

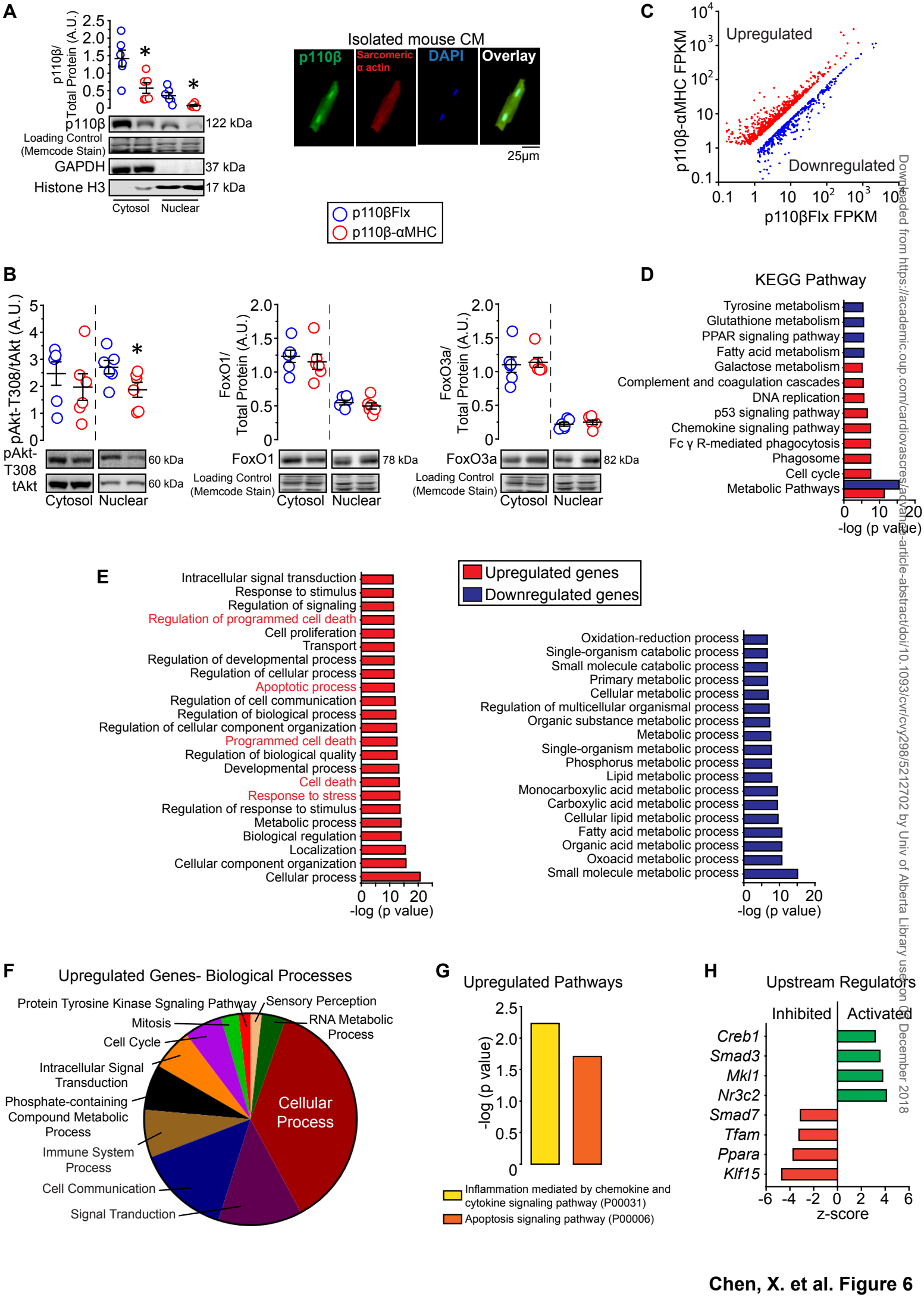

Chen, X. et al. Figure 6

Figure 7

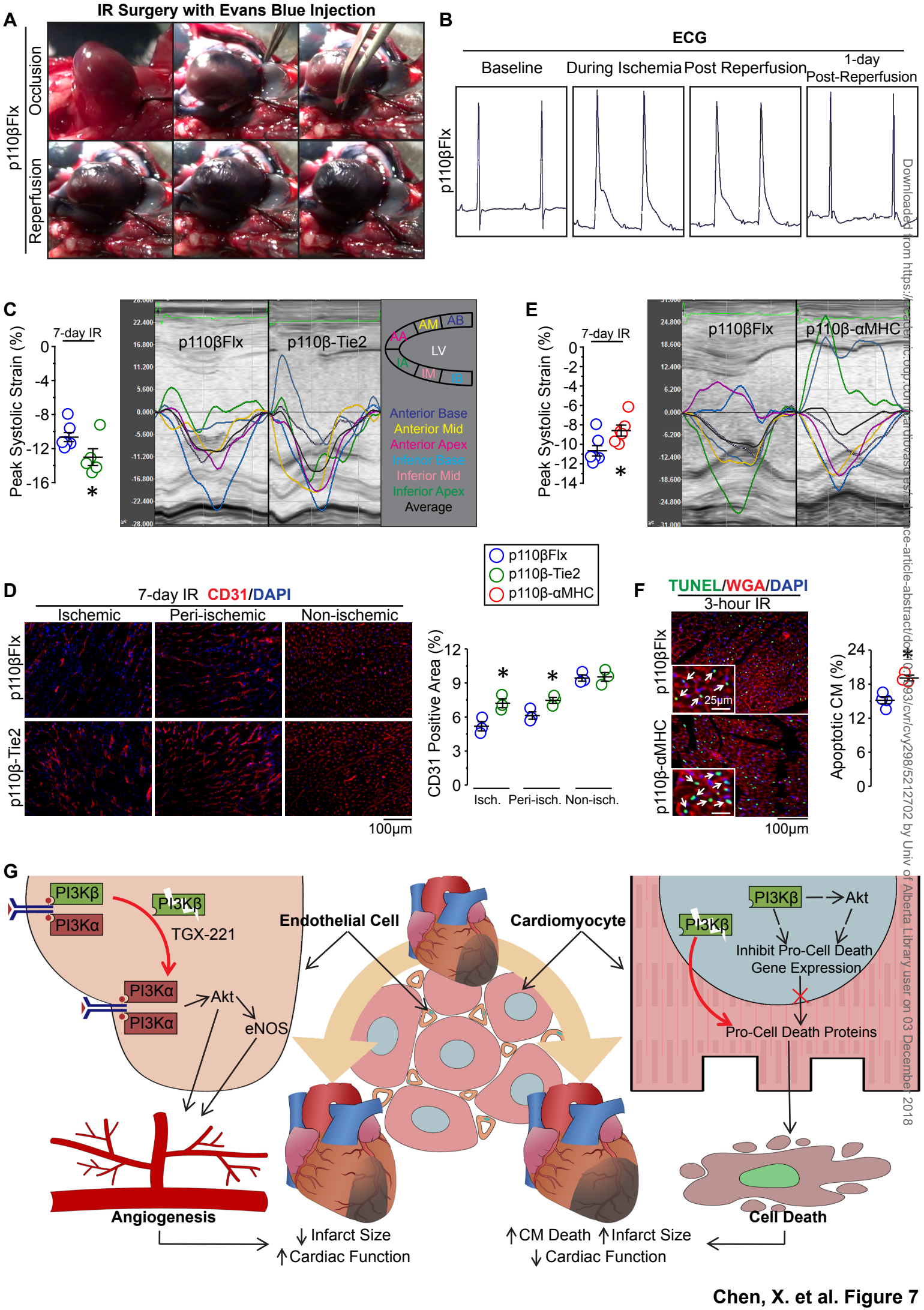

Chen, X. et al. Figure 7